An Investigation of the Environment of Some Aromatic Alcohol Solubilized Aqueous Ionic Micellar Solutions by Proton Magnetic Resonance Spectroscopy

Jong Jae Chung*, Jung-Bu Kang, Kyung Hee Lee, and Byung Il Seo

**Department of Chemistry, College of Natural Sciences, Kyungpook National University, Taegu 702-701*
Agency for Defense Development, Yuseong P. O. Box 35, Taejon 305-600

Received August 13, 1993

Chemical shifts in aqueous sodium dodecylsulfate(SDS) micellar solution solublizing phenol, catechol, resorcinol, hydroquinone have been measured to investigate solubilization properties. Proton nuclear magnetic resonance frequencies of solubilizates as well as those of the α-methylene, middle methylene and terminal methyl of SDS shift linearly as a function of solubilizate concentration. From the plots of observed chemical shift (ν) *vs* solubilizate concentration, slope (*a*) and solubilizate free chemical shift(ν_o) are obtained. They are very informative to solubilization site of the systems. Catechol and phenol solubilized SDS and catechol solubilized dodecylpyridinium chloride(DPC), dodecyltrimethylammonium bromide(DTAB) systems are studied using the same method to compare head group effect and middle methylene proton signal splitting. It is proposed that phenol and catechol are inserted into micellar interior and the number of methylenes assigned to the higher field peaks is 5.0±0.5.

Introduction

Since Eriksson[1] applied NMR to study solubilization of benzene and bromobenzene in cetyltrimethylammonium bromide(CTAB) solutions, many investigators have used NMR to study solublized systems. Eriksson and Gillberg[2] expanded their work to the solution of cyclohexane, isopropylbenzene, benzene, N,N-dimethylaniline, and nitrobenzene in CTAB. They surveyed the ^{1}H-chemical shift of solubilizate and CTAB and suggested the position of solubilizate molecules in the micellar systems. At low benzene concentrations in CTAB micelles, benzene resides mainly on the surface of the micelle whereas isopropylbenzene appears to be inside the core. At high concentration, however, solubilization in the interior was suggested. Recently, Rao *et al.*[3] proposed a mechanism for the origin of viscoelasticity of their CTAB-sodium salicylate/sodium *m*-chlorobenzoate/*m*-hydroxybenzoic acid system by high resolution FT-NMR studies. When any molecules are incorporated or solubilized in micellar solutions, they distribute themselves between the micellar and water phase in a particular location and direction. Different solubilized species can have different locations or orientation in micelle.[4,5,9] In this work some solutions of phenol and dihydroxybenzenes (catechol, resorcinol, hydroquinone) have been studied in aqueous ionic surfactants, such as sodium dodecylsulfate(SDS), dodecyltrimethylammonium bromide (DTAB) and dodecylpyridinium chloride(DPC) micellar systems of high concentration, well above the critical micelle concentration(CMC) by observing the ^{1}H-chemical shifts and middle methylene peak splitting. The role of the size of hydrophilic portion of aqueous surfactants on its solubilization ability has been studied by several workers.[6-10] Klevens[8] discussed the effect of the structure of the solubilizer on solubilization ability, but he mentioned very little about the nature of the hydrophilic portion of the molecule, "The cationic detergents, such as dodecylamine hydrochloride, are more powerful solubilizers for hydrocarbons than the corresponding anionic of equal chain length". And several workers[11-14] reported the splitting of the ^{1}H-NMR signal of middle methylene protons upon addition of certain aromatic compounds. The analysis of the location, distribution, and orientation of these species is getting more attention for better understanding of the equilibrium or kinetic aspects of the solubilization process itself and the physical and chemical behavior of the solubilized species.

This paper describes the structure of aromatic alcohol solubilizied in micelles by investigating the chemical shifts, α values, and methylene peak splitting phenomena.

Experimental

The chemicals used in this study were purchased from Aldrich, Merck, and Sigma company and purified using established techniques.[15] SDS, DTAB, DPC were recrystallized twice from ethyl acetate and washed with ethyl ether in Soxhlet extractor for 10 hours. Catechol, resorcinol, phenol and hydroquinone were recrystallized twice from benzene and methylene chloride. The ^{1}H-NMR spectra were obtained on Varian Associates FT-80A and Bruker AC300F spectrometer equipped with a variable temperature accessory. All spectra were taken at the constant temperature controlled within ± 0.5℃ in freshly prepared deuterium oxide (Aldrich 99.8%) solution and were measured relative to tetramethylsilane (TMS) contained in a coaxial capillary tube (Wilmad glass co) as an external standard. The resonance frequency of solvent water (HOD) in D_2O relative to the standard exhibited a negligible shift over the experimental solublizate concentration ranges, within ± 0.5 Hz.

Results and Disscusion

Solubilizate Effect. The ^{1}H-NMR resonance frequenc-

Table 1. ^{1}H-chemical Shifts of Solubilizates and SDS in D_2O Solution at 80 MHz and 40℃

Solubilizate	C_{SOL}*, M	Solubilizate			$SO_4C\underline{H}_2$	$CH_3(C\underline{H}_2)_n$**		$C\underline{H}_3(CH_2)_n$
Phenol		Ortho	Meta	Para				
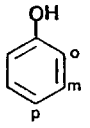	0.00				323.00	106.00		73.33
	0.05	548.30	577.60	554.57	321.41	103.88		71.90
	0.10	548.96	577.96	555.41	321.76	103.64		72.93
	0.20	547.07	575.89	553.85	319.33	101.71	99.31	72.35
	0.24	546.42	575.04	553.20	318.27	101.60	96.92	72.36
	0.48	542.83	572.55	550.49	313.84	101.73	87.19	73.57
	0.72	540.23	568.54	547.79	310.69	102.43	81.04	74.31
	0.96	537.87	565.74	545.09	308.25	101.74	76.26	73.87
	1.19	535.74	563.11	542.86	306.60	99.90	72.02	72.51
	2.39	532.91	552.90	535.08	304.25	86.90	65.19	58.33
Catechol		−a	−b					
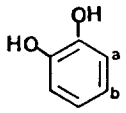	0.00				324.60	107.10		74.10
	0.02	549.80	545.80		324.40	106.40		73.50
	0.05	549.20	545.22		322.20	105.80		72.80
	0.10	548.50	544.52		321.10	103.40		72.00
	0.20	547.20	543.30		318.02	100.86		71.31
	0.40	545.30	541.70		315.90	100.20	94.40	71.00
	0.60	543.70	540.10		313.80	100.00	90.20	71.10
	0.80	542.10	535.80		311.90	99.50	87.00	70.80
	1.00	540.30	537.70		310.50	99.33	84.74	71.02
	1.50	537.60	533.60		308.30	98.50	80.50	69.90
Resocinol		−a	−b					
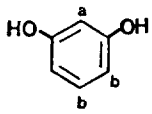	0.00				324.27	108.02		74.48
	0.04	570.06	513.48		324.29	106.63		73.60
	0.08	569.63	513.50		323.50	105.23		72.81
	0.16	568.90	512.96		323.46	102.88		71.42
	0.20	568.93	512.97		323.37	102.20		71.20
	0.40	566.62	511.02		321.65	98.53		68.93
	0.60	564.52	509.28		320.42	96.22		68.06
	0.80	562.22	507.42		319.11	93.76		66.78
	1.00	559.28	505.54		317.89	91.37		65.49
	1.50	552.61	500.33		314.58	85.78		61.76
	2.00	547.42	495.63		310.93	80.12		57.35
Hydroquinone		−a						
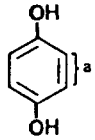	0.00				324.40	107.90		74.40
	0.02	544.52			324.34	107.34		73.98
	0.05	544.33			324.35	106.37		73.24
	0.10	543.84			324.20	104.79		72.02
	0.20	542.52			324.02	101.86		69.92
	0.40	540.83			323.42	99.03		68.05
	0.60	539.03			322.76	97.03		66.60
	0.80	536.39			321.64	94.51		64.81

*Solubilizate concentration M, **Splittd into two peaks in phenol and catechol aqueous micellar solution.

ies for 0.20 M SDS and those for phenol, catechol, resorcinol, hydroquinone are given in Table 1 and Figure 1. Increasing solubilizate concentration results in upfield shift of SDS protons except middle methylene and terminal methyl protons in case of phenol (dotted line in Figure 1). The difference in chemical shift for the SDS protons from 0.0 to 2.40 M phenol is in the order $CH_3(C\underline{H}_2)_9$(40.8 Hz)≫$SO_4C\underline{H}_2$(18.7 Hz)>$C\underline{H}_3(CH_2)_9$ (15.0 Hz) and phenol proton is in the order of *meta*-H>*para*-H>*ortho*-H. In the case of catechol, SDS proton shift is the same order as the phenol solutions over the similar concentration range, whereas those for resorcinol and hydroquinone are $CH_3(C\underline{H}_2)_9$ (27.9 Hz)>$C\underline{H}_3(CH_2)_9$ (17.1 Hz)>$SO_4C\underline{H}_2$ (13.3 Hz) and $CH_3(C\underline{H}_2)_9$ (13.4 Hz)>$C\underline{H}_3(CH_2)_9$ (9.6 Hz)>$SO_4C\underline{H}_2$ (2.8 Hz) respectively. The change of chem-

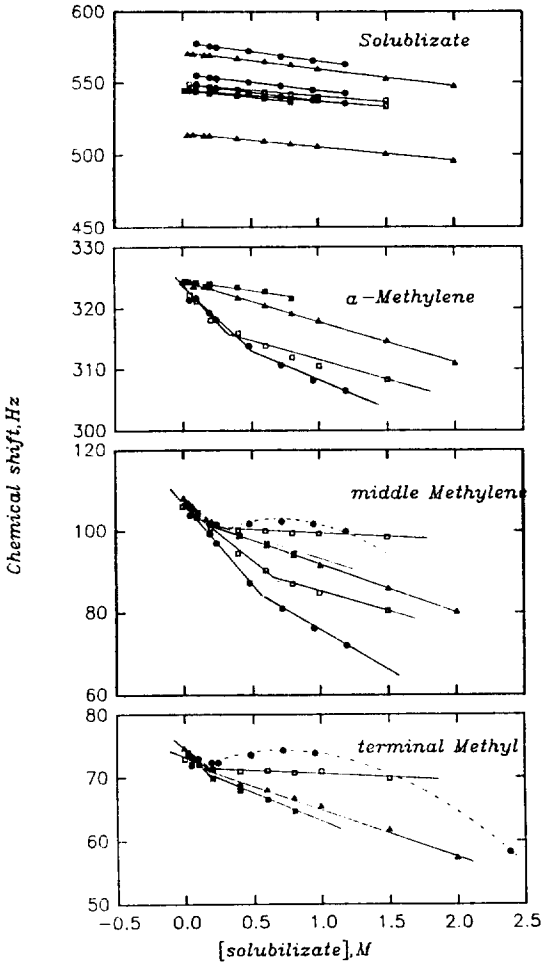

Figure 1. Chemical shifts of SDS protons as a function of solubilizate concentration in D_2O at 40℃, SDS concentration 0.2 M. ○ in phenol, ▲ in resorcinol, □ in catechol, ■ in hydroquinone.

ical shifts of SDS and solubilizate as a function of the solubilizate concentration is shown in Figure 1. At higher concentrations of phenol and catechol, the middle methylene of SDS splits into two peaks; the up-field and down-field signals were assigned to the methylenes close to the α-methylene of SDS and the methylene close to the terminal methyl, respectively. In Figure 1 the resonance signals of SDS exhibit a minor discontinuity in the region near 0.5 M solubilizate concentration, and those for solubilizates are linear all over the concentration range.

Eriksson and Gillberg,[2,16] reported similar discontinuities in CTAB-benzene, nitrobenzene systems. These breaks in plots of the observed chemical shifts as a function of solubilizate concentration were interpreted as a change in the solubilization site of the aromatic solubilizate in CTAB micelles. At a concentration of less than 1.0 M of benzene per mole of CTAB, benzene was proposed to be solubilized by adsorption at the micelle-water interface. At higher benzene concentration which correspond to the discontinuities in the plots of the resonance frequencies for the N-CH_3, -$(CH_2)_n$-, and α-CH_2 protons as a function of solubilizate concentration, adsorption saturation occurs and benzene and nitrobenzene are suggested to be located in the interior.[16] At higher concentrations of hydrocarbon additives or organic substrates, the size and shape of the micelle structure is clearly perturbed. In our present work, the observed discontinuities in the plots of chemical shift for the SDS protons as a function of increasing solubilizate concentration are due to the change in the micelle structure, such as size, shape, and/or water content. At the constant surfactant concentration, the chemical shift changes linearly within given concentration ranges as expressed by equation 1.

$$\nu = \nu_o + a[X] \quad (1)$$

Where ν is the observed chemical shift, ν_o is the chemical shift in the absence of solubilizate, $[X]$ is the concentration of solubilizate or substrate, and a is the slope.

Some investigators,[2,17-19] applied equation 1 to their surfactants-solubilizate system to study aromatic molecule-solubilized microstructures and to the surfactant-salt systems.[18,20] The changes in the orders of the difference in chemical shifts and splitting of middle methylene signals by the solubilizate structure imply that aqueous SDS micelle solubilized an aromatic alcohol is affected greatly in its structure. We applied equation 1 to our systems to compare this effect quantitatively. The obtained a and ν_o values are given in Table 2. The slope of plots of the observed chemical shifts for the surfactant or solubilizate protons *vs* the concentration of the added solubilizate give important information on the structure of micelle. Negative a values, resulting from the upfield shifts of the resonance frequencies are indicative of mutual shielding of the surfactants and aromatic protons, *i.e.*, a negative contribution to the local magnetic field by the aromatic ring. The initial slopes of the middle methylenes of the phenol and catechol solubilized SDS micellar solutions, are −36.3 (for phenol) and −31.7 (for catechol). However, the initial a values for the protons of the head groups, CH_2SO_4 (phenol; −17.2, catechol; −33.0) are more negative in the case of catechol. The negative a values for near the head group protons suggest that both catechol and phenol are solubilized predominantly in the region of the charged surface of the SDS micelle also catechol is "buried" more deeply. From the splitting of the middle methylene proton signals of SDS in aqueous phenol and catechol solutions, it is clear that the solubilizate molecule penetrates into the SDS micellar core. However, resorcinol and hydroquinone molecule doesn't split the middle methylene proton signals of SDS but broadens the resonance signals as the solubilizate concentration increases. Protons located above an aromatic ring are shift upfield by the ring current of the aromatic ring and protons at the side of the ring are shifted to the opposite direction. This suggests that some of middle methylene and terminal methyl protons of SDS in phenol are situated at the edge of the phenyl group. We will discuss the splitting of the middle methylene signal more quantitatively later.

Head Group Effect. The proton chemical shifts as a function of catechol concentration and a values obtained from equation 1 for catechol-SDS, DTAB, DPC systems are given in Tables 3 and 4.

The proton chemical shifts of α-methylene, middle methylene and terminal methyl of SDS and DPC and those of N-methyl, middle methylene of DTAB linearly increase in

Table 2. ^{1}H-NMR Parameter for Some Solubilizates in Aqueous SDS Micellar Solutions

[CT][a] range		Catachol[b] H-a	H-b	$SO_4C\underline{H}_2$	SDS $CH_3(C\underline{H}_2)_n$	$C\underline{H}_3(CH_2)_n$
0.00-0.20	*a*	−13.3	−12.7	−33.0	−31.7**	−11.6
	ν_o	549.8	545.8	324.5	107.0	73.5
[PhOH] range		Phenol o-H	m-H	p-H	SDS $SO_4C\underline{H}_2$	$CH_3(C\underline{H}_2)_n$	$C\underline{H}_3(CH_2)_n$
0.00-0.72	*a*	−13.3	−11.3	−11.9	−17.2	−36.3*	−6.2
	ν_o	578.6	556.1	549.3	322.6	106.0	73.3
[ROL] range		Resorcinol H-a	H-b	$SO_4C\underline{H}_2$	SDS $CH_3(C\underline{H}_2)_n$	$C\underline{H}_3(CH_2)_n$
0.00-0.20	*a*	−7.5	−3.9	−4.7	−2.0	−15.5
	ν_o	570.3	513.7	324.2	107.6	74.1
[HQ] range		Hydroquinone H-HQ		$SO_4C\underline{H}_2$	SDS $CH_3(C\underline{H}_2)_n$	$C\underline{H}_3(CH_2)_n$
0.00-0.20	*a*	−11.4		−1.92	−30.4	−22.5
	ν_o	544.9		324.4	107.9	74.4

*Higher field methylene, **Lower field methylene. [a]Solubilizate concentration, M. [b]a, b denotes the positions of protons (see Table 1).

Table 3. ^{1}H-chemical Shifts of Catechol and SDS, DTAB, DPC in D_2O Micellar Solution at 40℃

Surfactant	[Catechol]	$\nu_{catechol}$,* Hz		$\nu_{surfactant}$, Hz			
SDS		a	b	$SO_4C\underline{H}_2$	$CH_3(C\underline{H}_2)_n$		$C\underline{H}_3(CH_2)_n$
	0.00			324.60	106.10		73.90
	0.02			324.40	106.40		73.50
	0.05	549.20	545.22	322.20	105.80		72.80
	0.10	548.50	544.52	321.10	103.40		72.00
	0.20	547.20	543.30	318.02	100.86		71.31
	0.40	545.30	541.70	315.90	100.20	94.30	71.00
	0.60	543.70	540.10	313.80	100.00	90.20	71.10
	0.80	542.10	538.50	311.90	99.50	87.00	70.80
	1.00	540.30	537.70	310.50	99.33	84.74	71.02
	1.50	537.60	533.60	308.30	98.50	80.50	69.90
DTAB				$N\text{-}C\underline{H}_3$	$CH_3(C\underline{H}_2)_n$		$C\underline{H}_3(CH_2)_n$
	0.00			259.17	119.39		78.08
	0.02	549.78	540.58	251.75	105.67		73.57
	0.05	549.78	540.98	247.87	105.13		74.10
	0.10	547.58	540.42	243.52	107.67	99.84	77.46
	0.20	545.23	539.40	232.54	110.39	88.01	80.51
	0.40	543.67	539.01	221.56	113.50	79.50	83.74
	0.60	542.49	538.66	214.55	114.62	70.92	84.92
	0.80	541.75	538.27	210.01	115.24	68.01	85.51
	1.00	540.78	537.41	205.98	115.17	64.74	85.44
	1.50	538.42	543.92	199.16	113.30	61.00	83.30
	2.00	534.43	529.97	192.34	108.19	53.50	75.84
DPC				$PyC\underline{H}_2$	$CH_3(C\underline{H}_2)_n$		$C\underline{H}_3(CH_2)_n$
	0.00			378.90	95.58		63.17
	0.04	532.56	543.60	375.68	96.73		65.19
	0.08	529.57	540.13	367.40	96.70		65.03
	0.16	530.18	540.31	360.02	95.08		67.91

0.20	529.69	539.23	353.80	99.23	92.21	69.98
0.40	529.61	537.64	336.23	103.87	86.39	74.58
0.60	529.77	536.79	325.16	106.27	81.87	77.00
0.80	529.85	536.21	316.58	107.67	73.20	78.23
1.00	529.73	535.69	310.43	108.24	73.06	78.61
1.50	528.85	534.39	301.48	107.48	71.72	77.55
2.00	526.63	531.82	295.35	104.51	68.32	74.39

[a,b] denotes the positions of proton (see Table 1).

Table 4. ^{1}H-NMR Parameter for Catechol and Surfactants in Aqueous SDS, DPC, DTAB Micellar Solutions

Surfactant		Catechol-proton*					Surfactant protons		
SDS		a	b				$SO_4C\underline{H}_2$	$CH_3(C\underline{H}_2)_9$	$C\underline{H}_3(CH_2)_9$
	a	−13.3	−12.7				−33.0	−31.7	−11.6
	ν_o	549.8	545.8				324.5	107.0	73.5
DPC		a	b	o-H	m-H	p-H	$PyC\underline{H}_2$	$CH_3(C\underline{H}_2)_9$	$C\underline{H}_3(CH_2)_9$
	a	−21.4	−12.8	−165.4	−80.6	−71.7	−126.3	−30.9	31.2
	ν_o	543.4	532.0	721.3	654.8	693.5	379.5	98.9	63.3
TAB		a	b				N-CH_3	$CH_3(C\underline{H}_2)_9$	$C\underline{H}_3(CH_2)_9$
	a	−27.1	−7.8				−105.1	−102.8	38.9
	ν_o	550.6	541.1				253.6	109.2	73.0

*[a,b] denotes the positions of protons (see Table 1).

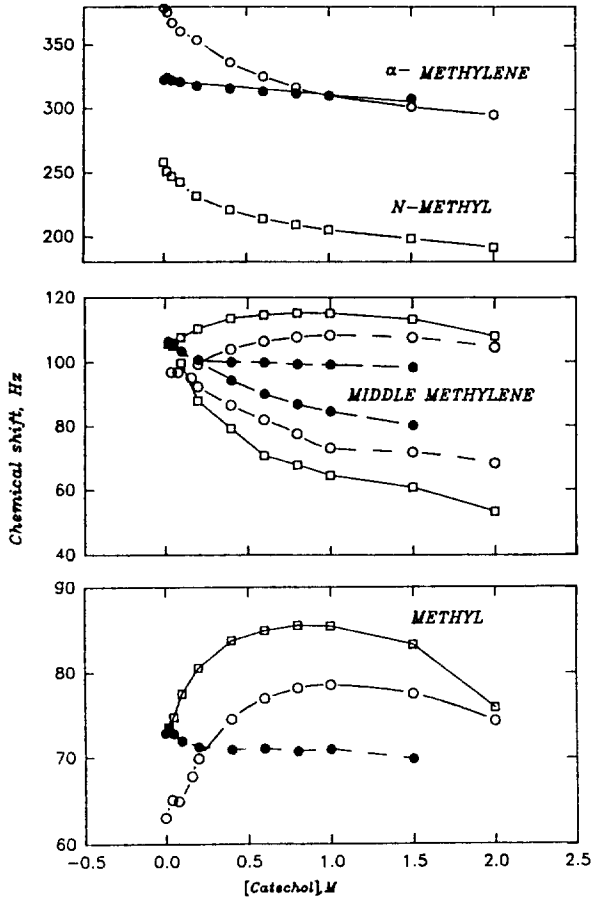

Figure 2. Chemical shift of catechol and SDS, DTAB, DPC in D_2O micellar solution at 40℃ (-●- SDS, -○- DPC, -□- DTAB).

the catechol concentration range of 0.0 to 0.20 M. In Figure 2 and Table 3, the order of the change of the chemical shift for α-CH_2 of surfactants is DPC (84.6 Hz)≫SDS (16.3 Hz) (that of DTAB couldn't obtained), for middle methylene, it is DTAB (84.6 Hz)≫DPC (27.3 Hz)≅SDS (25.6 Hz) and for terminal methyl only the chemical shift of SDS is upfield direction. On the plots of the cationic surfactants, DTAB and DPC, peaks are observed in the solubilizate concentration range of 0.8-1.0 M, where the middle methylene resonance signal begin to split. (Figure 2) We suppose that the methyl groups of DTAB and DPC are located in an edge direction of the phenyl group. Gratzel *et al.*[12] reported the downfield shift of the terminal methyl signal at their pyrene solubilized surfactants system. Their observation was explained by these kinds of protons are situated in an edge directly to the aromatic ring of the additive. Middle methylene groups in DPC and DTAB micellar solution, attached to terminal methyl group shifted to lower-field in the 0.8-1.0 M catechol concentration range. But in SDS micellar solution, they didn't shift any direction. This means that surfactant head group makes an important role in solubilization. It may be supposed that cationic surfactants have more shielding effect in aromatic alcohol solubilizied aqueous micellar solution. We need some additional experiments to explain the head group effect quantitatively. For α-methylene and middle methylene protons, *a* vlaues are ordered DPC>DTAB>SDS but those of terminal methyl are DTAB>DPC>SDS. From the results, we conclude that catechol is inserted deeper in cationic surfactants than in anionic surfactants. McBain and Hutchinson[4] said in their study on the effect of the ionic nature of the solubilizer, "It appears, in summary, that the difference between different types of materials containing the same long

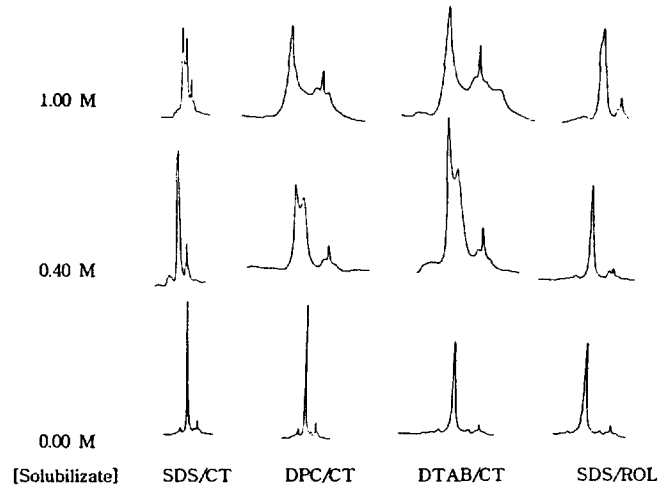

Figure 3. Methylene resonance of 0.2 M SDS, DPC, and DTAB at 80 MHz and 40℃ in the presence of various concentration of solubilizates (CT: catechol, ROL: resorcinol).

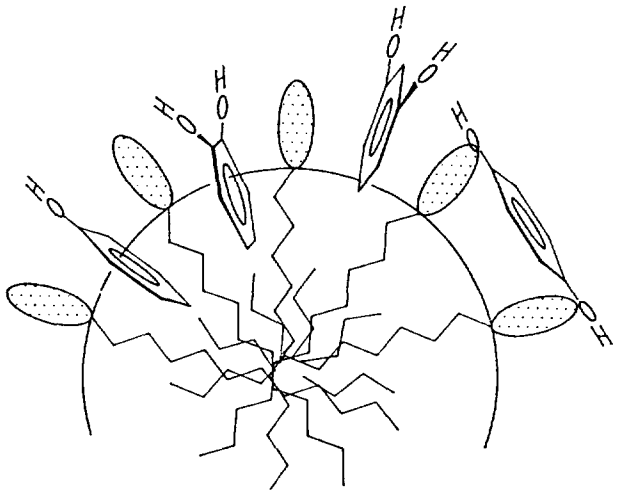

Figure 4. A proposed schematic representation of general solubilization sites of solubilizates (⬭: head groups of ionic surfactant).

Table 5. The Number of the Methylene Units Assigned to Higher- and Lower-field Split Peaks

Surfactant	SDS		SDS		SD*[a]		SDoS*[b]		DTAB		DPC	
Solubilizate	Phenol		Catechol		Phenol		Phenol		Catechol		Catechol	
CH_2 units**	High	Low	High	Low	High	Low	High	Low	High	Low	High	Low
	4.8	4.2	5.3	3.7	5.1	2.9	5.2	3.8	5.0	4.0	5.4	3.6

[a] Sodium dodecanoate. [b] Sodium dodecanosulfonate. *Taken from data in ref. 25. **The number of methylenes belong to higher field peaks was assigned based on the intensities of the split peaks.

chain hydrocarbon are relatively small, and that such differences as do exist may be explained in terms of the differences in the size of micelles formed by the various species", And Harris[10] discussed, "For compounds with equal equivalent carbon chain lengths, the degree of solubilization is the same. An exception is the cationic type, which seems to provide an increased degree of solubilization over anionics". We conclude that the solubilization ability of these surfactants is not simply related to the size parameter but these results are a little informative to propose a microstructure of the system.

The Middle Methylene Peak Splitting. We observe another important phenomena, the peak splitting of the middle methylene signals which was also reported for normal alkanes[21] and ethyl alkanoates[22] in aromatic solvents. Upon addition of catechol and phenol to the SDS micellar solution, the long methylene resonance begins to resolve into two well-defined peaks at the solubilizate concentration of *ca.* 0.20 M. Fendler *et al.*[13] reported that the initial splitting point of methylene protons is accompained by an increase in half-height line width ($\nu_{1/2}$) and by a qualitative increase in viscosity in their CTAB, SDS, 3-(dimethyldodecylamino)propane-1-sulfonate, and Igepal CO-730-acetophenone, -benzophenone system. Broadening of the middle methylene signal was not due to an increase in viscosity because other signals didn't broaden. The solubilizate concentration dependence suggests that at low concentration range, solubilizate is adsorbed closest to the Sterm layer of spherical micelle, at higher solubilizate concentration solubilizate penetrate more deeply into the micellar core and shields the methylene protons effectively. In Figure 3 the shape of splitted methylene peaks of surfactants in catechol and resorcinol are shown.

In the preceding discussion, it is clear that aromatic solubilizate is located parallel to the surfactants molecules in the palisade portion of the micelle, consequently, the splitting of the methylene signal in the ^{1}H-NMR spectra could be ascribed to shielding by large diamagnetic susceptibility of the aromatic ring of the solubilizates. Miyagishi *et al.*[23] reported that methylene peak splitting was observed only when the aromatic solubilizate had a moderate hydrophilic-lipophilic balance. Resorcinol and hydroquinone may be out of this balance range. Now, we propose a rough schematic diagram depicting the orientation of solubilizates on the micellar surface in Figure 4. Ulmius *et al.*[14], Miyagishi *et al.*[24] and Takashi *et al.*[25] reported the assignment of the split methylene signals of the ^{1}H-NMR spectra in CTAB, SDS, sodium alkanoate and sodium alkanosulfonates. Table 5 shows the results and comparison with Takashi *et al.*[24] There are little difference in the number of the methylenes assigned to the high-field peaks varying with the surfactant head groups. The numbers of the methylenes assigned to the high-filed peaks (5 ± 0.5) corresponds to the shielded part of the alkyl chain more strongly than other protons as a results of the magnetic anisotropy produced by the aromatic solubilizates. These results agreed with those of Takashi *et al.*,[25] but it's not quantitative. Now we are studying that kind of assignment by interpretation of ^{13}C-^{1}H correlation 2D-NMR.

References

1. Eriksson, J. C. *Acta. Chem. Scand.* **1963**, *17*, 1478.
2. Eriksson, J. C.; Gillberg, G. *Acta. Chem. Scand.* **1966**, *20*, 2019.
3. Rao, U. R. K.; Manohar, C.; Valaulikar, B. S.; Iyer, R. M. *J. Phys. Chem.* **1987**, *91*, 3286.
4. McBain M. E. L.; Hutchinson, E. *Solubilization and Related Phenomena*; Academic Press: New York, 1955.
5. Mittal K. L.; Mukerjee, P. *Micellization, Solubilization, and Microemulsion*; Plenum Press: New York, N. Y., 1977; Vol. 1, p 71.
6. Venable, R. L.; Nauman, R. V. *J. Phys. Chem.* **1964**, *68*, 3498.
7. McBain, J. W.; Richards, P. H. *Ind. Eng. Chem.* **1946**, *38*, 642.
8. Klevens, H. B. *Chem. Rev.* **1950**, *47*, 1.
9. Elworthy, P. H.; Florence, A. T.; Macfarlane, C. B. *Solubilization by Surface Active Agents*; Chapman and Hall Ltd.: London, **1968**.
10. Harris, J. C. *J. Am. Oil Chemists' Soc.* **1958**, *35*, 428.
11. Bunton, C. A.; Minch, M. J.; Midalgo, J.; Sepulveda, L. *J. Amer. Chem. Soc.* **1973**, *95*, 3262.
12. Grätzel, M.; Kalynasundaram, K.; Thoma, J. K. *J. Amer. Chem. Soc.* **1974**, *96*, 7869.
13. Fendler, J. H.; Fendler, E. J.; Infante, G. A.; Shih, P. S.; Patterson, L. K. *J. Amer. Chem. Soc.* **1975**, *97*, 89.
14. Ulmius, J.; Lindman, B.; Lindblom, G.; Drakerbert, T. *J. Colloid Interface Sci.* **1978**, *65*, 88.
15. Fendler, E. J.; Fendler, J. H. *Advan. Phys. Org. Chem.* **1970**, *8*, 271.
16. Eriksson, J. C.; Gillberg, G. *Surface Chem.* **1965**, *148*, 000.
17. Fendler, E. J.; Day, C. L.; Fendler, J. H. *J. Phys. Chem.* **1972**, *76*, 1460.
18. Gordon, J. E.; Robertson, J. C.; Thorne, R. L. *J. Phys. Chem.* **1970**, *74*, 957.
19. Fendler, J. H.; Fendler, E. J. *Catalysis in micellar and macromolecular system*; Chap 2, Academic Press: London, **1975**.
20. Muller, N.; Brikhann, R. H. *J. Phys. Chem.* **1967**, *71*, 957.
21. Liu, K. J. *J. Polym. Sci.* **1967**, *part A-2*, 5.
22. Liu, K. J. *Polymer* **1969**, *10*, 951.
23. Miyagishi, S.; Nishida, M. *J. Colloid Interface Sci.* **1980**, *78*, 270.
24. Miyagishi, S.; Nishida, M. *J. Colloid Interface Sci.* **1980**, *78*, 195.
25. Takashi, H.; Yoshio, I. *Bull. Chem. Soc. Jpn.* **1990**, *63*, 502.

Catalytic and Stoichiometric Hydroacylation of Olefin Derivatives with 8-Quinolinecarboxaldehyde by Rh(I)

Chul-Ho Jun*, Jong-Soo Han†, Jung-Bu Kang†, and Sun-Il Kim‡

Department of Chemistry, Yonsei University, Seoul 120-749
†Agnecy for Defense Development, P. O. Box 35, Taejon 305-600
‡Department of Chemical Engineering, Chosun University, Kwangju 501-759

Received September 16, 1993

Catalytic hydroacylation has been achieved by the reaction of 8-quinolinecarboxaldehyde (**1**) and various vinyl derivatives such as **2a**, **2b** and **2c** with Wilkinson's complex (**3**) to give linear alkyl ketones, **4a**, **4b** and **4c**, respectively. However, stoichiometric ligand-promoted hydroacylation of **2a** and **2b** with $[(C_8H_{14})_2RhCl]_2$ (**5**) resulted in a mixture of the branched alkyl ketones and the linear alkyl ketones in different ratios. Stoichiometric hydroacylation of some other olefin derivatives such as **6**, **11**, **12** and **26**, produced functionalized alkyl ketone compounds.

Introduction

The activation of C-H bond by transition metals is one of current interests in organometallic chemistry.[1] Especially, aldehydic C-H bond cleavage and its application to organic synthesis of ketone through hydroacylation have received much interest.[2] One major limitation for this process is decarbonylation.[3] There are some ways to overcome this limitation; for example, pressurizing the reaction with carbon monoxide or using special aldehyde such as 8-quinolinecarboxaldehyde and 2-iminopicoline systems which can cyclometallate the catalyst. Although carbon monoxide pressure retards decarbonylation of the acylmetal hydride intermediate formed from the aldehydic C-H bond cleavage by metal complexes, the reaction still requires vigorous conditions.[4] 8-Quinolinecarboxaldehyde is a good cyclometallation substrate, since it does not show any decarbonylation due to its formation of the stable 5-membered metallacyclic complex.[5]

As a model study for hydrometallation through C-H bond activation, hydroacylation has been applied to many different reactions such as C-C bond cleavage of the strained ring molecule,[6] synthesis of β, γ-unsaturated ketones,[7] and the elucidation of olefin isomerization mechanism.[8] Recently, catalytic hydroacylation of α, ω-diene has been repored.[9] In this paper, we report the results of the catalytic hydroacylation and the stoichiometric ligand-promoted hydroacylation